A flow cytometer-based method to simultaneously assess activity and selectivity of compounds against the intracellular forms of *Trypanosoma cruzi*

Cristian Gabriel Miranda[a], Maria Elisa Solana[a], Maria de los Angeles Curto[b], Estela Maria Lammel[a], Alejandro Gabriel Schijman[b], Catalina Dirney Alba Soto[a],*

[a] Facultad de Medicina, Instituto de Investigaciones en Microbiología y Parasitología Médicas (IMPaM),UBA-CONICET, Universidad de Buenos, Paraguay 2155, Ciudad Autónoma de Buenos Aires CC1121ABG, Argentina
[b] Laboratorio de Biología Molecular de la Enfermedad de Chagas, Instituto de Investigaciones en Ingeniería Genética y Biología Molecular (INGEBI-CONICET), Vuelta de Obligado 2490 Piso 2, Ciudad Autónoma de Buenos Aires C1428ADN, Argentina

A R T I C L E   I N F O

A B S T R A C T

Chagas disease is a major unsolved health issue in Latin America and an emerging threat worldwide. New drugs are urgently needed for chemotherapy as those available (benznidazole and nifurtimox) have variable efficacy and elevated toxicity. Efforts are actually oriented to improve tools and technologies (*e.g.* transgenic parasites, flow cytometry or image-based systems) for the screening of large numbers of candidate compounds for their activity against *Trypanosoma cruzi* (*T. cruzi*). Methods that test drug efficacy and selectivity in the same assay are suitable to accelerate the process of drug discovery. Here, we developed a GFP expressing *T. cruzi* from a moderate virulence stock and confirmed that the transgenic parasite retained the biological characteristics of the parental strain. With this tool, we established a flow cytometer-based method to simultaneously test drug activity against intracellular amastigotes and toxicity to the host cell. This one-step procedure allows determining the selectivity index of the tested compound in a sensitive and accurate manner even with low infection rates. This method can provide additional information on the interactions between drug, parasites and host cell and could be adapted to other trypanosomatids and protozoa with intracellular multiplication.

© 2015 Elsevier B.V. All rights reserved.

1. Introduction

The protozoan parasite *Trypanosoma cruzi* is the causative agent of Chagas disease. At least 8 million people in Latin America are infected with *T. cruzi* and, per year, 13,000 of them die as a result. Chagas disease is a major health problem and a leading cause of cardiopathy in the region (Moncayo and Silveira, 2009). Migration of infected patients to urban centers all over the world has changed the former rural scenario of the disease. Chagas disease is emergent in regions where the vector is not present owing to non-vectorial routes including congenital transmission or blood transfusion and solid organ transplantation from infected donors (Chatelain, 2015). At present, epidemiological models estimate that 300,000 infected people reside in the United States more than 100,000 in Europe, 1500 in Australia and 3000 in Japan (WHO, 2011).

As no vaccines against the parasite disease are currently available, chemotherapy is necessary not only to alleviate clinical manifestations but also as to reduce parasite transmission. Pharmacological treatment of Chagas disease is actually based on the administration of two heterocyclic compounds: benznidazole and nifurtimox. These drugs show significant efficacy (80%) when administered during the acute infection with the best results obtained in pediatric patients (Viotti et al., 2009; Urbina, 2010). However, their efficacy decays when administered at the chronic stage of infection and their diverse side effects are often associated with poor patient compliance (Guedes et al., 2011; Coura, 2009). The discovery of more effective and safer therapeutic compounds is necessary to cover all stages of the infection (Urbina, 2010; Chatelain, 2015). New systems to evaluate compound efficacy and selectivity in accurate and reproducible manner are required (Romanha et al., 2010; Chatelain, 2015; Bustamante and Tarleton, 2011).

The activity of novel compounds is often initially explored on the replicative stage present in the insect vector (epimastigote) in view of its availability in axenic cultures. However, the informa-

tion obtained cannot always be extrapolated to the parasite stages present in the mammalian hosts (Romanha et al., 2010). Currently, the use of trypomastigote and amastigote stages for the screening of new compounds is unquestionable. The assessment of inhibitory activity against the amastigote stage is even more relevant as it provides information about the efficacy of a new compound over the duplicative stage in humans. It also informs about the interaction with the host cell that may limit the intracytoplasmic drug availability or promote cell toxicity. In early stages of development, *in vitro* cytotoxicity of candidate compounds is usually tested in parallel assays by measuring metabolic activity of viable mammalian cells or by dye exclusion or uptake tests. Yet, in the case of intracellular pathogens one must take into account that any apparent inhibitory activity of a candidate drug can be the result of host cell damage after exposure to the compound. An ideal assay should screen compound's cytotoxicity using as target the infected host cell. In fact, the final goal of *in vitro* testing is to prove that selective pathogen inhibition can be achieved at concentrations unable to produce toxic effects to the host cell. For that reason, the selectivity index (CC50/IC50) is calculated as a predictor of a compound's therapeutic window.

Transgenic parasites have greatly facilitated the screening of antiparasitic compounds (Canavaci et al., 2010; Kessler et al., 2013; Goyard et al., 2014; Andriani et al., 2011). Reporter gene technology is more sensitive than classical methods for detection and quantitation of low numbers of intracellular parasites. The pTREX vector was developed and optimized to achieve stable expression of these genes in *T. cruzi* and other trypanosomatids (Vazquez and Levin, 1999). It integrates at the ribosomal promoter locus by homologous recombination and allows the overexpression of foreign genes (Lorenzi et al., 2003). Still, a concern with transgenic parasites is whether insertion and expression of foreign genes can modify their fitness compared to the parental *T. cruzi* isolate.

In this work we developed a transgenic *T. cruzi* that stably expresses GFP during its life cycle and in successive passages *in vivo* and *in vitro*. We confirmed that integration of the pTREX vector and expression of foreign genes does not compromise the main biological characteristics of the parental strain. With this transgenic parasite we set up a flow cytometry-based method to test the activity of novel compounds against the intracellular amastigote that all together monitors toxicity against the host cell.

2. Materials and methods

2.1. Parasites

K98 *T. cruzi* strain (a clone derived by limiting dilution from the CA-I isolate; González Cappa et al., 1980) and the transgenic K98 GFP strain were kept by serial intraperitoneal passage in CF1 mice every 6 weeks with an inoculum of 1×10^5 trypomastigotes. To obtain trypomastigotes for *in vitro* culture, bloodstream forms were purified from blood of infected mice. Briefly the blood was diluted with PBS-3% fetal calf serum (FCS) at a 1:5 ratio. After centrifugation for 10 min at $300 \times g$ the sample was incubated at 37 °C for 1 h. The supernatant was then harvested – excluding the erythrocyte containing phase – and spun for 30 min at $10,000 \times g$ to recover the pellet containing parasites. *T. cruzi* epimastigotes were routinely maintained in axenic culture at 28 °C in liver infusion tryptose (LIT) media supplemented with 10% fetal calf serum, 20 μg/ml haemin, 100 μg/ml of streptomycin and 100 U/ml of penicillin.

2.2. Generation of K98 GFP transgenic epimastigotes

Epimastigotes were harvested at exponential phase after 48 hs of culture by centrifugation at $3000 \times g$ for 10 min at room temperature. Following pellet washing in PBS, 1×10^8 parasites

were suspended in 350 μl of electroporation buffer (PBS 1×, MgCl$_2$ 0.5 mM, CaCl$_2$ 0.1 mM) and mixed with 10–15 μg of the transfection vector pTREXgfp DNA. Parasite suspension was electroporated in 0.2 cm gap cuvettes with a discharge of 400 V 500 μF, yielding time constants varying between 3.5 and 5 ms. Parasites were then diluted in 5 ml of LIT and incubated at 28 °C for 48 h to allow recovery before the addition of 100 μg/ml of G418 (Sigma). Following 7–10 days of incubation, mock-transfected parasites completely stopped dividing and resistant parasites were incubated in the presence of G418 for another two weeks before cloning by serial dilution in 96-well plates. Only stable cell lines were used through this work. The insertion of the vector at the ribosomal locus was confirmed by PCR using total genomic DNA from transfected parasites as template and the T7 (TAATACGACTCACTATAGGG) and RibDS (GTGTGTACTTGTGCGCAT) primers used under the following conditions: 94 °C, 3 min; 94 °C, 30 s, 55 °C, 30 s, 72 °C, 1 min, 40 cycles; 72 °C, 10 min. Stationary phase transgenic epimastigotes were differentiated to metacyclic trypomastigotes by culture in modified Grace medium supplemented with 10% FCS and haemin (Isola y col., 1986). Cultures containing metacyclic trypomastigotes were used to infect Vero cells or to infect mice.

2.3. Animals and T. cruzi *infection*

Balb/c and CF1 mice were bred and housed at the animal facilities of the IMPaM (UBA-CONICET). Mice were kept under standard conditions on a 12-hour light, 12-hour dark cycle in a temperature controlled room (25 ± 2 °C) with food and water ad libitum. All animal procedures were approved by institutional regulations of the Committee for the Care and Use of Laboratory Animals (approval No. RS2079/2007, Universidad de Buenos Aires) and were in accordance with government regulations of the National Food Safety and Quality Service (SENASA, resolution No. RS617/2002, Argentina). All efforts were made to minimize the number of animals used and their suffering. Age and sex matched mice were infected by intraperitoneal route with an inoculum of 1×10^5 bloodstream forms of the K98 GFP and K98 wild type (WT) *T. cruzi* strains. Weight was recorded periodically and peripheral blood parasitemia was measured by counting, in a Neubauer chamber, the number of parasites obtained from the tail vein blood diluted (1/10) in red blood cell lysis solution (Tris–NH$_4$ Cl 0.83% pH 7.2).

2.4. Determination of T. cruzi-*specific antibodies*

Antibody levels in serum were determined by ELISA following standard procedures. ELISA plates were coated with *T. cruzi* epimastigote-whole lysate (15 μg/well) in carbonate/bicarbonate buffer (pH 9.6) and incubated overnight at 4 °C wells. After blockade with 5% low fat milk for 1 h at 37 °C, plates were washed with PBS-0.01% Tween 20^{TM} (Sigma, St. Louis, USA). Sera were diluted and incubated for 2 h at 37 °C. Plates were washed five times with PBS-0.01% Tween 20^{TM} and incubated with 1/5000 polyclonal goat anti-mouse IgG-peroxidase conjugate (Sigma, St. Louis, MO, USA) in PBS for 1 h at 37 °C. The reaction was developed with *o*-phenylenediamine (Sigma, St. Louis, USA) 0.4% in citrate buffer (24 mM citrate, 58 mM Na$_2$HPO$_4$·2H$_2$O, pH 5.2) and 5 μl hydrogen peroxide 0.4 mg/ml and stopped with 1 N H$_2$SO$_4$. Optical densities were measured at 492 nm in a plate reader.

2.5. Histopathological analysis

Heart and skeletal muscle tissues (quadriceps) were fixed in 10% formaline. Paraffin-embedded tissue sections were stained with hematoxylin and eosin and evaluated for the presence of tissue damage and parasite nests. Four non-consecutive slides of each tissue sample were analyzed in a blind fashion. The number of
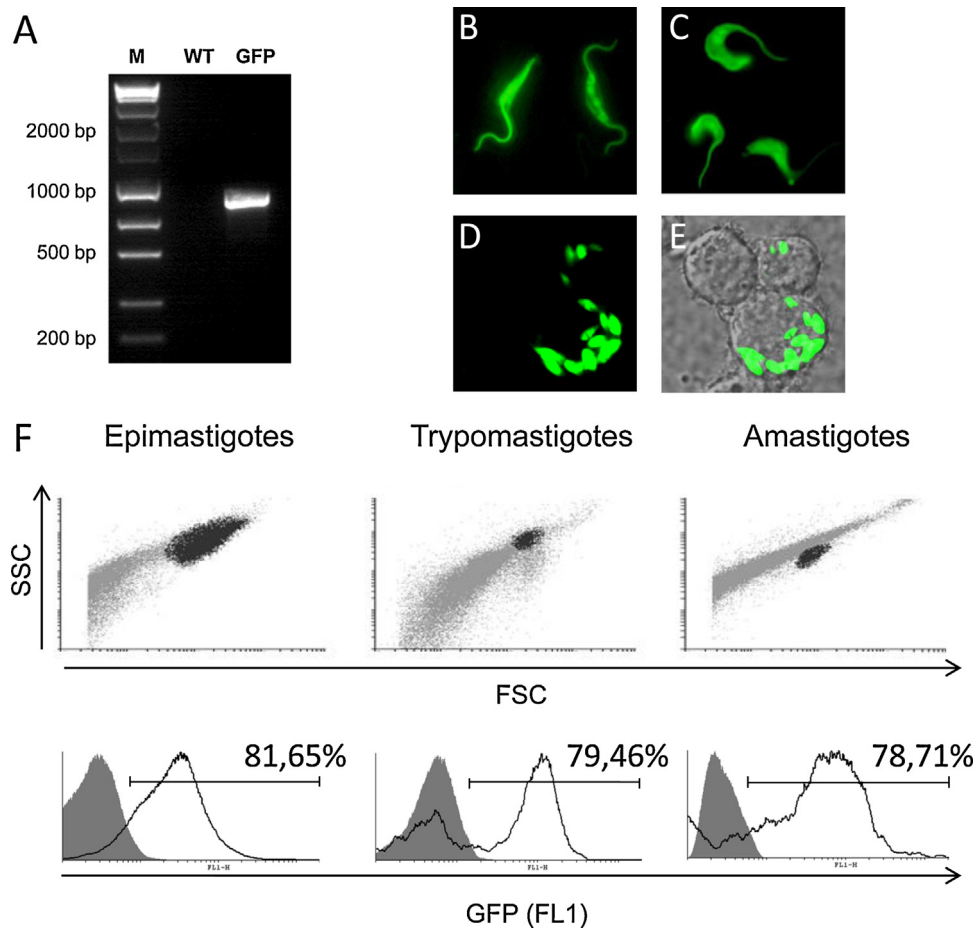
Fig. 1. Generation of a transgenic *T. cruzi* K98 strain that stably expresses GFP. Confirmation of pTREX vector integration into the *T. cruzi* genome by PCR using T7 and RiBDS primers that recognize specific sequences for the pTREX and *T. cruzi* ribosomal promoter region respectively. PCR was performed with genomic DNA from non-transfected (WT) and transgenic (GFP) parasites (A). Expression of GFP by the major stages of the K98 GFP transgenic strain were visualized under fluorescence microscope: axenic epimastigotes (B), purified bloodstream trypomastigotes (C) and *in vitro* cultured intracellular amastigotes (D). Merged fluorescence and differential interference contrast of intracellular amastigotes cultured in Vero cell monolayers (E). Representative flow cytometry scatter plots of the gating regions for axenic epimastigotes, enriched bloodstream trypomastigotes and *in vitro* cultured amastigotes are shown (F top). Overlay histograms of FL1 (GFP) fluorescence of each parasite stage from the K98 GFP (black line) and native (solid grey) *T. cruzi* strains (F bottom).

focal inflammatory infiltrates per observed field was determined to obtain a qualitative measure of tissue damage (expressed as number of inflammatory foci over total number of observed fields). To obtain a quantitative measure of tissue damage a digital image of each inflammatory focus was obtained using a Nikon ECLIPSE E600 microscope. An area containing each inflammatory infiltrate was created and the number of pixels contained in the selection was counted using the Image J software (NIH, USA) as a direct measure of the size of the inflammatory focus.

2.6. Quantitation of parasite burden in tissues by qPCR

In brief, tissue specimens were separately subjected to lysis in a buffer containing 50 mM Tris [pH 8] (Promega, USA), 10 mM EDTA (Promega), 100 mM NaCl (Sigma), 1% [w/v] SDS (Promega) and 300 μg/ml proteinase K (Promega). Samples were heated for 2 h at 55 °C and DNA was purified by phenol extraction followed by ethanol precipitation. For PCR reaction, the *T. cruzi* satellite nuclear repeat was amplified with primers SatFw (5′-GCAGTCGGCKGATCGTTTTCG-3′) and SatRv (5′-TTCAGRGTTGTTTGGTGTCCAGTG-3′). The 20 μl reaction tube contained 0.5 μM of primers Sat Fw and Sat Rv, 3 mM MgCl₂, 250 μM of each dNTP, 0.5 U of Platinum Taq polymerase (Invitrogen, Life Technologies, USA), EvaGreen (Bio-Rad Laboratories,

USA) at a final concentration of 0.5× and 2 μl of sample DNA. Thermal cycling comprised an initial denaturation step of 5 min 95 °C, followed by 40 cycles of 94 °C for 15 s, 59 °C for 15 s and 72 °C for 15 s on a 7500 Real Time PCR System (Applied Biosystems). In a separate PCR reaction, the single copy murine-specific TNF-α gene was amplified in each sample using primers TNF-5241 (5′-TCCCTCTCATCAGTTCTATGGCCCA-3′) and TNF-5411 (5′-CAGCAAGCATCTATGCACTTAGACCCC-3′) at a final concentration of 1 μM. All other PCR reagents and cycling conditions were the same as for the *T. cruzi* satellite DNA amplification. For normalization between tissue samples, the concentration of *T cruzi* satellite DNA obtained for each sample was corrected with that obtained for the TNF-α gene amplification. A standard curve of parasite-spiked host tissue DNA was generated as follows. 50 mg of tissue were collected from control mice, minced and spiked with 2×10^7 epimastigotes. DNA was extracted as described above. The same process was carried out to extract DNA from 50 mg of tissue from control mice. Then DNA was serially tenth-fold diluted with host DNA to generate a standard curve that contained 2×10^5–2×10^{-2} parasite equivalents per 50 ng of total DNA as measured by spectrophotometer (Nanodrop, Thermo Fisher Scientific). The CT value of each sample in duplicate was interpolated in the standard curve to calculate the parasite equivalents per 50 ng of total DNA.
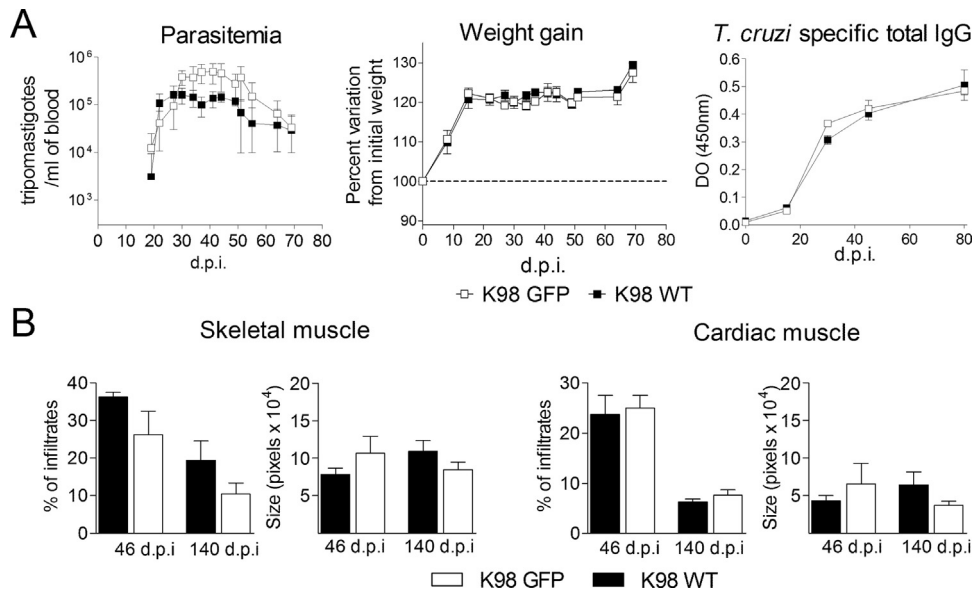
Fig. 2. Transgenic K98 GFP *T. cruzi* strain retains the biological characteristics of the parental strain. Six week old Balb/c mice ($n = 5$) were infected by intraperitoneal route with 1×10^5 bloodstream trypomastigotes from K98 WT and K98 GFP strains of *T. cruzi*. The kinetics of parasitemia, weight gain and *T. cruzi* specific IgG production by K98 GFP (white squares) and K98 WT (black squares) infected mice was recorded (A). Tissue damage was analyzed in H&E stained paraffinic embedded sections of skeletal muscle (quadriceps) and hearts of infected animals. The frequency of inflammatory infiltrates (% of infiltrates) and the average size of infiltrates at two different times post infection were recorded as described in material and methods (B). Data are shown as the mean ± SEM.

2.7. In vivo evaluation of T. cruzi susceptibility to benznidazole

Mice were infected with 10^5 trypomastigotes by intraperitoneal route and treated with benznidazole (Bz, Radanil®, Roche) 120 mg/kg/day for 30 days starting on day 12, time when infection was confirmed by microhematocrit (Feilij et al., 1983). Drug tablets were crushed in a mortar and suspended in corn oil. Each mouse received 0.20 ml of the suspension by oral gavage using an18-gauge stainless animal feeding needle (Thomas Scientific, Swedesboro, NJ, USA). Parasitemia levels were recorded in mice infected with K98 GFP or K98 WT and treated with Bz as well as untreated animals.

2.8. In vitro evaluation of drug activity against bloodstream trypomastigotes

Trypomastigotes obtained from mice at the peak of parasitemia were purified from peripheral blood as described previously (Dolcini et al., 2008). Parasites (2.5×10^5 per well) were cultured at 37 °C in 5% CO_2 atmosphere in RPMI supplemented with 5% FCS in 96 well plate in triplicate in the presence of increasing concentrations of Bz (range = 0.362–60 μg/ml). Tablets were pulverized and dissolved in DMSO. After 24 h viable motile parasites were counted by light microscopy in a Neubauer chamber. Controls consisted in RPMI supplemented with 5% FCS as well as RPMI plus 0.5% of DMSO.

2.9. In vitro evaluation of drug activity against intracellular amastigotes and host cell toxicity

For flow cytometry analysis J774 cells were seeded in RPMI1640 supplemented with 5% FCS at 5×10^4 cells per well in 96-well plates. After 1 h of incubation at 37 °C and with a 5% CO_2 atmosphere, trypomastigotes were added at MOI of 1:5 (cell: trypomastigote). Three hours later, cells were washed with RPMI to remove trypomastigotes that failed to enter cells and increasing doses of freshly prepared dilutions (0.362–60 μg/ml) of Bz or (0.05–500 μg/ml) of an allopurinol derivative (compound H) or (0.0462–100 μg/ml) amphotericin B in sodium deoxycholate (Cat 1672348, ICN). In all cases the medium containing the drug was renewed daily. After 72 h of treatment the cells were harvested with a Trypsin/EDTA solution and processed for FACS analysis. In experiments using propidium iodide (PI) (Sigma, St. Louis, USA), it was added to cell suspensions (5 μg/ml) 10 min prior to FACS acquisition in a Partec PAS III flow cytometer (Partec GmbH, Münster, Germany). J774 cells were recognized by their FSC *vs* SSC properties and autofluorescence at the FL1 and FL2 channels was evaluated in cultured untreated cells. Amastigote-infected cells were identified in the FL1 channel. Cells that incorporated PI were detected in the FL2 channel. A total of 20,000 events were acquired for each sample. Data analysis was performed using Cyflogic software (CyFlo Ltd.). For Giemsa staining assay J774 cells were fixed in methanol and stained with 10% v/v of Giemsa solution (pH 7). Stained coverslips were then washed with tap water and mounted for microscopy. The number of infected host cells was recorded in at least 400 host cells, in duplicate experiments. Results were expressed as the inhibition of intracellular amastigote growth. Control cultures were incubated in medium alone or with equal DMSO concentrations. The IC50 value (the drug concentration that inhibits 50% of parasite growth) and CC50 (the drug concentration that exerts cytotoxicity on 50% of host cells) was calculated by non-linear regression using the GraphPad prism version 5.00 for Windows (San Diego, CA, USA).

2.10. Statistics

Data were expressed as means ± SEM. The Mann–Whitney test was used for comparisons between two groups. F test was used for dose response curve comparisons. A value of $p < 0.05$ was considered significant. Tests were performed using the GraphPad prism version 5.00 for Windows (San Diego, CA, USA).

3. Results

3.1. Characterization of the transgenic T. cruzi K98 GFP strain

The pTREXgfp vector was used to transfect the epimastigote stage of the K98 *T. cruzi* parasites. Plasmid integration at

the ribosomal promoter of the *T. cruzi* genome was established by PCR amplification (Fig. 1A). GFP protein expression by transfected parasites was confirmed in epimastigotes, trypomastigotes and intracellular amastigote stages by fluorescence microscopy (Fig. 1B–E). Flow cytometry revealed that transfected parasites retained the morphometric profiles (size and complexity) of the parental strain. The fluorescence intensity was homogeneous in all parasitic stages evaluated. Nearly 80% of the parasites expressed the GFP reporter gene in absence of drug selection in all stages (Fig. 1F). The fitness and stability of the fluorescent parasite population was assessed *in vitro* during successive passages on axenic epimastigotes as wells as on trypomastigotes and amastigotes cultured in Vero cells monolayers. The percentage of fluorescent bloodstream trypomastigotes found in *T. cruzi* infected mice was uniformly around 80% all over the acute phase of infection and has remained stable for 3 years during successive passages through mice (Data not shown).

3.2. K98 GFP retains the biological characteristics of the parental strain

The parental K98 *T.cruzi* strain belongs to the discrete typing unit (DTU) TcI (Burgos et al., 2013) and displays a preferential tropism for skeletal and cardiac muscles. Being non-lethal at the acute infection, even at high inoculum, infected mice reach the chronic phase (Mirkin et al., 1994; González Cappa et al., 1980). We assessed whether the transgenic K98 GFP displayed the biological properties of the parental K98 strain. Parasitemia levels, body weight variation and anti-*T. cruzi* IgG production were similar between mice infected with K98 GFP and WT strains (Fig. 2A). Moreover both strains displayed the same tissue tropism and histopathologic features (Fig. 2B).

We also analyzed *in vitro* and *in vivo* susceptibility of the transgenic strain to the reference drug benznidazole (Bz). Mice infected with K98 GFP and WT and subsequently treated with Bz showed undetectable levels of parasitemia by conventional microscopy at the end of the therapy (Fig 3a). Parasite load in target tissues was significantly reduced ($p < 0.05$) when compared to that of untreated controls (Fig. 3B). Susceptibility to different concentrations of Bz was also tested *in vitro* on K98 GFP and K98 WT trypomastigotes. Dose-response curves were generated with the transgenic and parental parasites. The *F* test for curve comparison showed no significant differences in the curve for both series of data. The IC50 values retrieved for Bz against K98 GFP and K98 WT were 3.8 μM (CI95% 1.87–8.02) and 5.3 μM (CI95% 1.36–21.24) respectively, Fig. 3C).

3.3. Flow cytometry-based evaluation of amastigote growth inhibition using the K98 GFP transgenic strain

We developed a flow cytometer based assay to test the inhibitory activity of compounds against the amastigote stage of a low virulence strain as the parental K98. For this purpose, J774 cells were infected with purified blood trypomastigotes at a MOI 1:5. After 72 h of Bz treatment, cells were analyzed by flow cytometry (Fig. 4A–C). Uninfected J774 cells showed no autofluorescence at the FL1 channel (Fig. 4B). Without drugs, the infectivity of trypomastigotes from the K98 GFP strain was lower than 14% in all assays permorfed (Fig. 4C). Yet, the homogeneous expression of GFP facilitated the detection by flow cytometry of small numbers of K98 GFP intracellular amastigotes. The activity of Bz against intracellular amastigotes was calculated at different drug concentrations to generate dose-response curves for the inhibitory activity of Bz (Fig. 4D and F). We compared results obtained by flow cytometry with those obtained with the conventional photomicroscopy-based method following Giemsa staining of cell
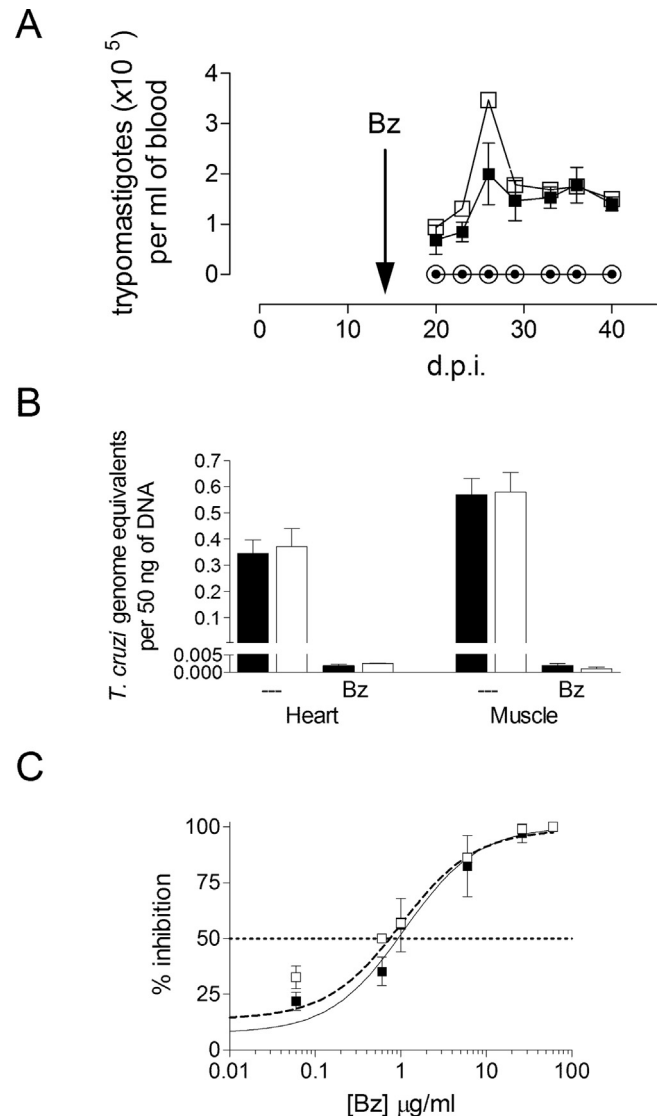

Fig. 3. *In vivo* and *in vitro* susceptibility to the reference drug benzidazole (Bz). Balb/c mice ($n = 5$) were infected with 1×10^5 trypomastigotes of K98-WT or K98-GFP strain and then treated with Bz 120 mg/kg/day by oral gavage for 30 days starting on day 12 after infection. Parasitemia levels were recorded in mice infected with K98 GFP and treated with Bz (white circles) or untreated (white squares) as well as those infected with the K98 WT and treated with Bz (black circles) or untreated (black squares) (A). Parasite burden in muscle and heart tissue of mice infected with K98 GFP (white squares) and K98 WT (black squares) treated or untreated with Bz. Tissue parasite burden was determined 45 days after infection by quantitative PCR as described in Section 2. Results are expressed as parasite genome equivalents per 50 ng of total DNA. The data show the mean ± SEM ($n = 3$). Student *t* test **$P < 0.01$; *$P < 0.05$ (B). The *in vitro* susceptibility to Bz of K98 GFP trypomastigotes was tested. Trypomastigotes purified from peripheral blood of mice infected with K98 GFP or WT strains of *T. cruzi* were cultured at 37 °C and 5% CO_2 for 24 h in RPMI supplemented with 5% FBS in the presence of different concentrations of Bz in triplicate. Dose-response curves generated for Bz inhibitory activity against trypomastigotes of K98 WT (black squares discontinuous line) and K98 GFP strains (white squares, solid line) are shown (C). Each point represents the mean of three replicates +/− SD.

cultures (Fig. 4E). Comparison of dose-responses curves retrieved for both assays with the *F* test showed no significant differences ($P = 0.1542$; $F = 2.07$). The IC50 values for Bz obtained with flow cytometry and conventional microscopy of Giemsa stained infected cells were 15.3 μM (CI95% 13.2–17.7) and 14.2 μM (CI95% 8.3–24.3) respectively (Fig. 4F).
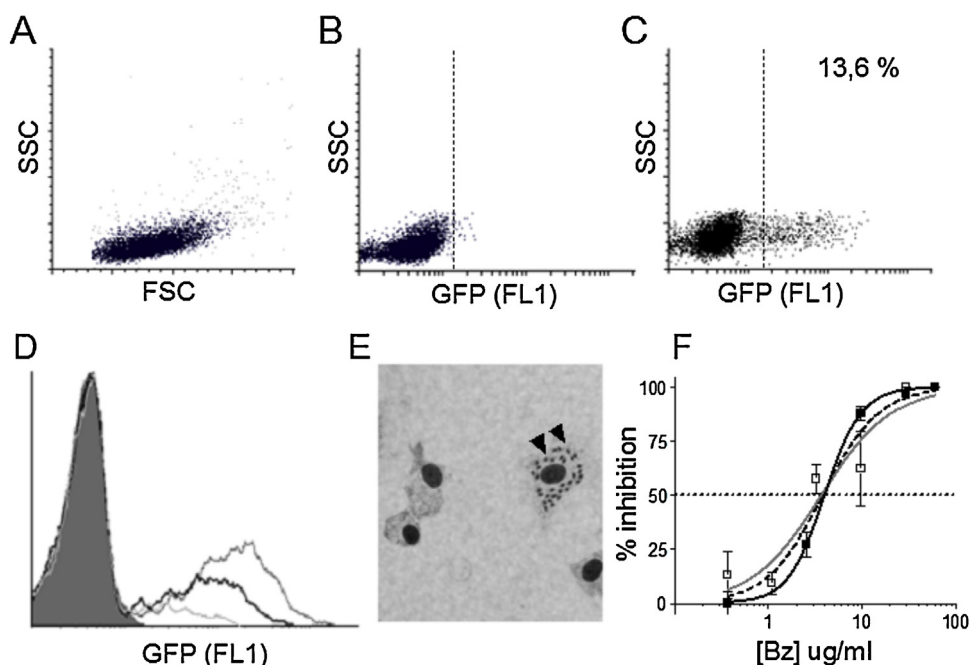
Fig. 4. *In vitro* screening of the inhibitory activity of intracellular amastigote growth using a fluorescent parasite strain displaying low infectivity. J774 cells were seeded at 5×10^4 cells per well in 96-well plates for the flow cytometry assay and 5×10^5 cells in sterile 12 mm round coverslips inserted in 24-well plates for the Giemsa staining assay. They were infected with K98 GFP at a MOI 1:5. After 72 h of culture in RPMI 5% FBS at 37 °C in 5% CO_2 cells were harvested to be acquired in a flow cytometer and coverslips were collected and colored with Giemsa staining for light microscopy count. A representative FSC *vs* SSC plot of J774 cells (A). A representative SSC *vs* FL1 channel of uninfected J774 cells (B). A representative SSC *vs* FL1 channel of J774 cells 72 h after infection with K98 GFP with the percent of GFP positive cells shown in the text box (C). Representative histograms showing the GFP expression by K98 GFP infected J774 cells following exposure for 72 h to different concentrations of Bz (light grey line: 9.8 μg/ml; black line: 2.5 μg/ml) and untreated control (grey line) (D). A representative microphotograph (400×) of Giemsa stained K98 GFP infected J774 cells. Black arrowheads indicate an infected cell harboring intracellular amastigotes. (E). Representative concentration-response curve obtained with microscopy and Giemsa staining methods (open squares, grey line), flow cytometry-based method (black boxes, black line) and the shared curve generated with both data sets (discontinuous line) are shown. Each point represents the mean of three replicates +/− SD. Curve comparison was performed with *F* test. ($P = 0.154$, $F = 2.08$) (F).

3.4. A combined flowcytometry- based method for the simultaneous determination of compounds activity against T. cruzi amastigotes and toxicity against the host cell

A method to test, in the same well, the inhibitory activity of a compound against the intracellular amastigote stage and the toxicity to the host cell was developed. The procedure was based on the selective binding of propidium iodide (PI) dye to nucleic acids of host cells whose plasma membrane had become permeable due to cell damage. Cytotoxicity was quantified by flow cytometry on the basis of host-cell counting and measure of their PI uptake. J774 cells infected with K98 GFP parasites were cultured for 72 h in the presence of different concentrations of Bz, Amphotericin B (Fungizone®) an antifungal with demonstrated activity against *T. cruzi*) and a synthetic compound (H) with unknown activity against the parasite. At the end of the assay, J774 cells were collected and PI was added to the cell suspension prior to acquisition. The frequency of *T. cruzi* K98 GFP infected cells was evaluated on the FL1 channel and cell viability loss (PI incorporation) on the FL2 channel. In cell suspensions where the J774 cell population could not be distinguished from cell debris at the forward scatter *vs.* side scatter plot by flow cytometry due to complete cell monolayer destruction, cytotoxicity was defined as 100%. The intrinsic fluorescence in the FL1 and FL2 channels of J774 cells is negligible (Fig. 5A left). In the absence of drugs, *T. cruzi* infected cells (FL1 positive cells expressing GFP) following 72 h of culture did not incorporate PI (Fig. 5A middle). In the presence of 50 μg/ml of the allopurinol derivative H, nonviable cells stained bright red (FL2) with PI were distinguishable from viable ones (Fig. 5A right). In these cell suspensions, no double positive events were detected probably reflecting the lack of parasite growth in nonviable cells. Drug dose-response curves of amastigote inhibitory activity and cell toxicity were generated

(Fig. 5B). The IC50 and the CC50 (drug concentration that affects viability of 50% of cells in culture) values were obtained to calculate the selectivity index (SI) for each drug according to the formula (SI = CC50/IC50). Consistent with previous reports in the literature, both Bz and Amphotericin B have the capacity to inhibit amastigote growth at doses showing no substantial toxicity to the host cell (Yardley and Croft, 1999). Nevertheless, as reflected by the selectivity index the therapeutic window of the reference drug Bz is wider than that of Amphotericin B. The method was also useful to determine that a synthetic compound H exhibited poor activity against the parasite with a selective index of 3.22 considerably below the acceptable threshold of 10 for a hit and 100 for a lead candidate compound against *T. cruzi* (Chatelain, 2015).

4. Discussion

We developed a transgenic fluorescent parasite strain from a low virulence *T.cruzi* isolate. Next, we established a procedure to evaluate selectivity index of a candidate compound by simultaneously measuring its activity against *T. cruzi* and cytotoxicity to the host cell. For this, we used PI a fluorescent molecule commonly used to exclude non-viable cells in multicolor flow-cytometry assays (Jones and Senft, 1985). PI is incorporated by the nucleus of cells whose plasma membranes have become permeable due to cell damage or death which usually occurs in late stages of apoptosis or during necrosis. We confirmed that *in vitro* infected host cells (GFP positive cells) have an intact membrane 72 h after infection. This finding indicates that PI incorporation is suitable to detect in an objective manner the loss of host cell membrane integrity caused by the off-target drug effects of tested compounds at a single cell level. With this assay, we assessed amastigote growth inhibitory activity and the therapeutic range of drugs with proved activity
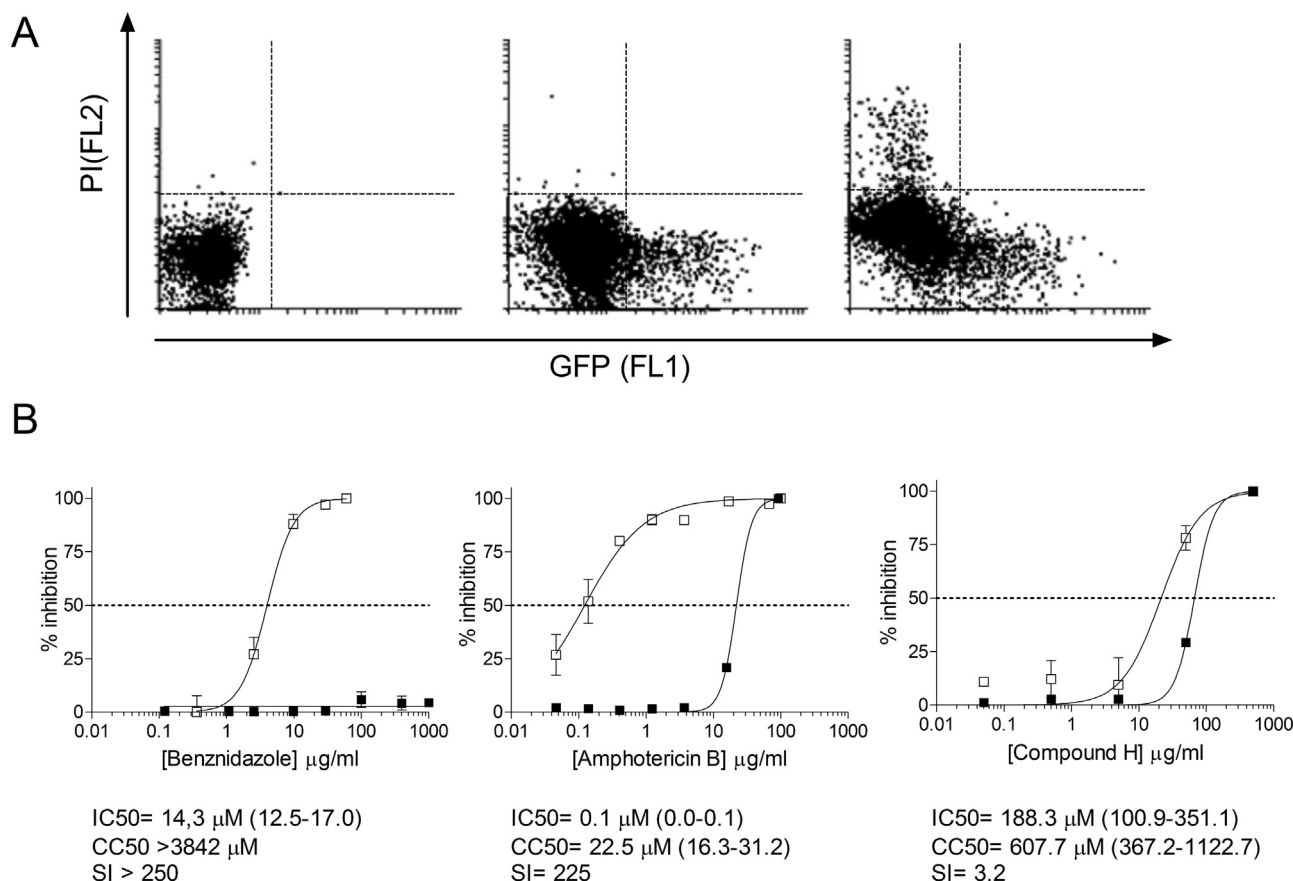
IC50= 14,3 μM (12.5-17.0)
CC50 >3842 μM
SI > 250

IC50= 0.1 μM (0.0-0.1)
CC50= 22.5 μM (16.3-31.2)
SI= 225

IC50= 188.3 μM (100.9-351.1)
CC50= 607.7 μM (367.2-1122.7)
SI= 3.2

Fig. 5. A combined flow cytometry-based method for the simultaneous determination of *in vitro* efficacy and toxicity of compounds against *T. cruzi* intracellular amastigotes. Representative scatter plots of the FL1 (GFP) and FL2 (propidium iodide) signals from uninfected J774 cells (left) and K98 GFP infected J774 cells untreated (middle) or treated with 50 μg/ml of the allopurinol derivative H (right) (A). Inhibition of K98 GFP amastigote growth (open squares) and cell toxicity (solid squares) on J774 cells in 96 well in the presence of drugs at different concentrations was determined on harvested cells by flow cytometry (B). Each point represents the mean of three replicates +/− SD. Inhibitory concentration 50% (IC50) and cytotoxic concentration 50% (CC50) are shown with their confidence intervals 95% in brackets. Selectivity index (SI) was calculated according to the formula: SI = CC50/IC50.

against the parasite as Bz, the reference drug, and amphotericin B. A novel synthetic compound was also tested that displayed a poor selectivity index. The flow cytometry-based assay to evaluate the *in vitro* inhibitory activity of drugs against amastigotes showed a good correlation with classical microscopy-based method with the advantage of counting large cells numbers in a fast, automated and reproducible manner. Even though flow cytometry has the disadvantage over fluorometer plate readers of only providing end-point data, it permits measuring different fluorescent signals on the same cell event. In our hands, as well as in recent reports, sensitivity of the fluorometer requires prolonged culture times, large amounts of fluorescent parasites or high infection rates that do not mimic physiological conditions (Rocha et al., 2013). The assay described here uses non-irradiated dividing cells and can be adapted to any cell type (*i.e.* myoblasts, loosely adherent or non-adherent cells).

A major goal of screening assays is to be scalable for high throughput screening. In recent years, fully automated image-based approaches have been developed and refined to screen for the activity of thousands of molecules against *T. cruzi* stocks or clinical isolates in short term informative assays (Moon et al., 2014; Engel et al., 2010; Alonso-Padilla et al., 2015). Some of them have been designed to simultaneously evaluate the toxicity of candidates by counting total host cell nuclei using DNA intercalating dyes on previously fixed cells. However, only cell nucleus disintegration, but not early stages of cell death process, can be assessed as a toxic effect of candidate drugs. PI combined with flow cytometry allows for the subtle distinction, without prior fixation, of live and dead cells that happen to be morphologically indistinguish-

able. This feature adds further sensitivity to the toxicity test. In addition the use of fluorescent parasites and PI dye minimize the manipulation steps prior to assay readout. Flow cytometry has long been recognized for its high speed analysis (>30,000 cells per second) multi-parameter and capabilities providing highly informative and statistically robust data using small cell suspension volumes. For this reasons, flow cytometry resources with automated microwell plate based sampling are being developed for pharmaceutical screening facilities making this assay scalable for high throughput/high content screening (Edwards and Sklar, 2015). Furthermore, the possibility of multiparameter analysis allows for the evaluation of additional markers on the host cell and/or the parasite related to the mode of action of the drug or the off-target effects (*i.e.* apoptosis, cell cycle arrest, altered metabolic pathways) thus giving further understanding on the interaction between drug, parasites and host cell.

For practical reasons, assays to test compounds *in vitro* are commonly performed using highly infective *T. cruzi* strains that exhibit elevated lethality during acute infection in the murine model. Yet, mice experimentally infected with natural *T. cruzi* isolates frequently exhibit features of chronic infection that better reproduces the course of human Chagas disease than these high-virulence strains (Marinho et al., 2009). It is relevant to develop reproducible and sensitive assays using *T. cruzi* strains of moderate virulence as the one used here.

Broad differences in biological properties among *T. cruzi* isolates have been recognized (Buscaglia and Di Noia, 2003; Alba Soto et al., 2003; Batalla et al., 2013). The wealth of *T. cruzi* genotypes and phe-

notypes are actually grouped into six DTU TcI-TcVI (Zingales et al., 2009). K98 strain belongs to the DTU TcI, a genotype that circulates at the present among human populations all over Latin America (Guhl and Ramírez, 2011; Cura et al., 2012). Being K98 a well characterized clone derived from a *T. cruzi* human isolate, its use might confer to assays advantages of monoclonal population structures such as homogeneity and reproducibility as recently proposed by Zingales et al. (2014). Further work is currently undergoing in order to build up a panel of low virulence recombinant parasites from other DTUs.

Even though pTREX is an overexpression vector widely used to transfect trypanosomatids, a comprehensive study has not been done to test whether integration and expression of foreign proteins could affect the biological characteristics of the parasite. Indeed, reports in the literature show that engineering of *T. cruzi* strains to express beta-galactosidase or fluorescent proteins can alter parameters as infectivity to mice compared to their parental strains (Le-Senne et al., 2002; Guevara et al., 2005; Santos et al., 2000). We confirmed here that integration of the pTREXgfp vector does not affect the fitness of the parasite *in vitro* or in the mouse model of infection, maintaining throughout its life cycle the fluorescent signal without need of further re-selection. It is frequently reported by other researchers in the field that a proportion of trypanosomatids transfected with integrative vectors randomly fail to express the reporter gene probably due to stochastic variations in the transcription and translation processes of the transgenic protozoan population (Taylor and Kelly, 2006; DaRocha et al., 2004; Pires et al., 2008). Sorting of fluorescent parasites by flow cytometry could remove non-GFP expressing parasites but the percent of fluorescent parasites consistently stabilizes around 80%, but not lower than this, after few generations.

The screening of the activity and selectivity of drug candidates presented here could be applied to other protozoa with intracellular life stages like *Leishmania* spp. or *Toxoplasma gondii* that have been already modified to express fluorescent proteins. Furthermore, the spectral characteristics of PI make this dye suitable for use in combination with different fluorescent proteins currently available.

Acknowledgements

References

Alba Soto, C.D., Mirkin, G.A., Solana, M.E., González Cappa, S.M., 2003. *Trypanosoma cruzi* infection modulates *in vivo* expression of major histocompatibility complex class II molecules on antigen-presenting cells and T-cell stimulatory activity of dendritic cells in a strain-dependent manner. Infect. Immun. 71 (3), 1194–1199.

Alonso-Padilla, J., Cotillo, I., Presa, J.L., Cantizani, J., Peña, I., Bardera, A.I., Martín, J.J., Rodriguez, A., 2015. Automated high-content assay for compounds selectively toxic to *Trypanosoma cruzi* in a myoblastic cell line. PLoS Negl. Trop. Dis. 9 (1), e0003493.

Andriani, G., Chessler, A.D., Courtemanche, G., Burleigh, B.A., Rodriguez, A., 2011. Activity *in vivo* of anti-*Trypanosoma cruzi* compounds selected from a high throughput screening. PLoS Negl. Trop. Dis. 5 (8), e1298.

Batalla, E.I., Pino Martínez, A.M., Poncini, C.V., Duffy, T., Schijman, A.G., González Cappa, S.M., Alba Soto, C.D., 2013. Impairment in natural killer cells editing of

immature dendritic cells by infection with a virulent *Trypanosoma cruzi* population. J. Innate. Immun. 5 (5), 494–504.

Burgos, J.M., Risso, M.G., Brenière, S.F., Barnabé, C., Campetella, O., Leguizamón, M.S., 2013. Differential distribution of genes encoding the virulence factor trans-sialidase along *Trypanosoma cruzi* discrete typing units. PLoS One 8 (3), e58967.

Buscaglia, C.A., Di Noia, J.M., 2003. *Trypanosoma cruzi* clonal diversity and the epidemiology of Chagas' disease. Microbes. Infect. 5 (5), 419–427.

Bustamante, J.M., Tarleton, R.L., 2011. Methodological advances in drug discovery for Chagas disease. Expert Opin. Drug Discov. 6 (6), 653–661.

Canavaci, A.M., Bustamante, J.M., Padilla, A.M., Perez Brandan, C.M., Simpson, L.J., Xu, D., Boehlke, C.L., Tarleton, R.L., 2010. *In vitro* and *in vivo* high-throughput assays for the testing of anti-*Trypanosoma cruzi* compounds. PLoS Negl. Trop. Dis. 4 (7), e740.

Chatelain, E., 2015. Chagas disease drug discovery: toward a new era. J. Biomol. Screen 20 (1), 22–35.

Coura, J.R., 2009. Present situation and new strategies for Chagas disease chemotherapy: a proposal. Mem. Inst. Oswaldo Cruz 104 (4), 549–554.

Cura, C.I., Lucero, R.H., Bisio, M., Oshiro, E., Formichelli, L.B., Burgos, J.M., Lejona, S., Brusés, B.L., Hernández, D.O., Severini, G.V., Velazquez, E., Duffy, T., Anchart, E., Lattes, R., Altcheh, J., Freilij, H., Diez, M., Nagel, C., Vigliano, C., Favaloro, L., Favaloro, R.R., Merino, D.E., Sosa-Estani, S., Schijman, A.G., 2012. *Trypanosoma cruzi* discrete typing units in Chagas disease patients from endemic and non-endemic regions of Argentina. Parasitology 139 (4), 516–521.

DaRocha, W.D., Silva, R.A., Bartholomeu, D.C., Pires, S.F., Freitas, J.M., Macedo, A.M., Vazquez, M.P., Levin, M.J., Teixeira, S.M., 2004. Expression of exogenous genes in *Trypanosoma cruzi*: improving vectors and electroporation protocols. Parasitol. Res. 92 (2), 113–120.

Dolcini, G.L., Solana, M.E., Andreani, G., Celentano, A.M., Parodi, L.M., Donato, A.M., Elissondo, N., González Cappa, S.M., Giavedoni, L.D., Martínez Peralta, L., 2008. *Trypanosoma cruzi* (Chagas' disease agent) reduces HIV-1 replication in human placenta. Retrovirology 5, 53.

Edwards, B.S., Sklar, L.A., 2015. Flow cytometry: impact on early drug discovery. J. Biomol. Screen 20 (6), 689–707.

Engel, J.C., Ang, K.K., Chen, S., Arkin, M.R., McKerrow, J.H., Doyle, P.S., 2010. Image-based high-throughput drug screening targeting the intracellular stage of *Trypanosoma cruzi*, the agent of Chagas' disease. Antimicrob. Agents Chemother. 54 (8), 3326–3334.

Feilij, H., Muller, L., Gonzalez Cappa, S.M., 1983. Direct micromethod for diagnosis of acute and congenital Chagas' disease. J. Clin. Microbiol. 18 (2), 327–330.

González Cappa, S.M., Chiale, P., del Prado, G.E., Katzin, A.M., de Martini, G.W., de Isola, E.D., Abramo Orrego, L., Segura, E.L., 1980. Isolation of a strain of *Trypanosoma cruzi* from a patient with chronic Chagas cardiomyopathy and its biological characterization. Medicina (B Aires) 40 (Suppl. 1), 63–68.

Goyard, S., Dutra, P.L., Deolindo, P., Autheman, D., D'Archivio, S., Minoprio, P., 2014. *In vivo* imaging of trypanosomes for a better assessment of host-parasite relationships and drug efficacy. Parasitol. Int. 63 (1), 260–268.

Guedes, P.M., Silva, G.K., Gutierrez, F.R., Silva, J.S., 2011. Current status of Chagas disease chemotherapy. Expert Rev. Anti Infect. Ther. 9 (5), 609–620.

Guevara, P., Dias, M., Rojas, A., Crisante, G., Abreu-Blanco, M.T., Umezawa, E., Vazquez, M., Levin, M., Añez, N., Ramirez, J.L., 2005. Expression of fluorescent genes in *Trypanosoma cruzi* and *Trypanosoma rangeli* (Kinetoplastida: Trypanosomatidae): its application to parasite-vector biology. J. Med. Entomol. 42 (1), 48–56.

Guhl, F., Ramírez, J.D., 2011. *Trypanosoma cruzi* I diversity: towards the need of genetic subdivision? Acta Trop. 119 (1), 1–4.

Jones, K.H., Senft, J.A., 1985. An improved method to determine cell viability by simultaneous staining with fluorescein diacetate-propidium iodide. J. Histochem. Cytochem. 33 (1), 77–79.

Kessler, R.L., Gradia, D.F., Pontello Rampazzo, R.e.C., Lourenço, É., Fidêncio, N.J., Manhaes, L., Probst, C.M., Ávila, A.R., Fragoso, A.P., 2013. Stage-regulated GFP expression in *Trypanosoma cruzi*: applications from host-parasite interactions to drug screening. PLoS One 8 (6), e67441.

Le-Senne, A., Muelas-Serrano, S., Fernández-Portillo, C., Escario, J.A., Gómez-Barrio, A., 2002. Biological characterization of a beta-galactosidase expressing clone of *Trypanosoma cruzi* CL strain. Mem. Inst. Oswaldo Cruz 97 (8), 1101–1105.

Lorenzi, H.A., Vazquez, M.P., Levin, M.J., 2003. Integration of expression vectors into the ribosomal locus of *Trypanosoma cruzi*. Gene 310, 91–99.

Marinho, C.R., Nuñez-Apaza, L.N., Bortoluci, K.R., Bombeiro, A.L., Bucci, D.Z., Grisotto, M.G., Sardinha, L.R., Jorquera, C.E., Lira, S., Lima, M.R., Alvarez, J.M., 2009. Infection by the Sylvio X10/4 clone of *Trypanosoma cruzi*: relevance of a low-virulence model of Chagas' disease. Microbes Infect. 11 (13), 1037–1045.

Mirkin, G.A., Jones, M., Sanz, O.P., Rey, R., Sica, R.E., González, C., appa, S.M., 1994. Experimental Chagas' disease: electrophysiology and cell composition of the neuromyopathic inflammatory lesions in mice infected with a myotropic and a pantropic strain of *Trypanosoma cruzi*. Clin. Immunol. Immunopathol. 73 (1), 69–79.

Moncayo, A., Silveira, A.C., 2009. Current epidemiological trends for Chagas disease in Latin America and future challenges in epidemiology, surveillance and health policy. Mem. Inst. Oswaldo Cruz 104 (Suppl. 1), 17–30.

Moon, S., Siqueira-Neto, J.L., Moraes, C.B., Yang, G., Kang, M., Freitas-Junior, L.H., Hansen, M.A., 2014. An image-based algorithm for precise and accurate high throughput assessment of drug activity against the human parasite *Trypanosoma cruzi*. PLoS One 9 (2), e87188.

Pires, S.F., DaRocha, W.D., Freitas, J.M., Oliveira, L.A., Kitten, G.T., Machado, C.R., Pena, S.D., Chiari, E., Macedo, A.M., Teixeira, S.M., 2008. Cell culture and animal

infection with distinct *Trypanosoma cruzi* strains expressing red and green fluorescent proteins. Int. J. Parasitol. 38 (3–4), 289–297.

Rocha, M.N., Corrêa, C.M., Melo, M.N., Beverley, S.M., Martins-Filho, O.A., Madureira, A.P., Soares, R.P., 2013. An alternative *in vitro* drug screening test using *Leishmania amazonensis* transfected with red fluorescent protein. Diagn. Microbiol. Infect. Dis. 75 (3), 282–291.

Romanha, A.J., Castro, S.L., Soeiro, M.e.N., Lannes-Vieira, J., Ribeiro, I., Talvani, A., Bourdin, B., Blum, B., Olivieri, B., Zani, C., Spadafora, C., Chiari, E., Chatelain, E., Chaves, G., Calzada, J.E., Bustamante, J.M., Freitas-Junior, L.H., Romero, L.I., Bahia, M.T., Lotrowska, M., Soares, M., Andrade, S.G., Armstrong, T., Degrave, W., Andrade, Z.e.A, 2010. *In vitro* and *in vivo* experimental models for drug screening and development for Chagas disease. Mem. Inst. Oswaldo Cruz 105 (2), 233–238.

Santos, W.G., Metcheva, I., Buck, G.A., 2000. Colony polymerase chain reaction of stably transfected *Trypanosoma cruzi* grown on solid medium. Mem. Inst. Oswaldo Cruz 95 (1), 111–114.

Taylor, M.C., Kelly, J.M., 2006. pTcINDEX: a stable tetracycline-regulated expression vector for *Trypanosoma cruzi*. BMC Biotechnol. 6, 32.

Urbina, J.A., 2010. Specific chemotherapy of Chagas disease: relevance, current limitations and new approaches. Acta Trop. 115 (1–2), 55–68.

Vazquez, M.P., Levin, M.J., 1999. Functional analysis of the intergenic regions of TcP2beta gene loci allowed the construction of an improved *Trypanosoma cruzi* expression vector. Gene 239 (2), 217–225.

Viotti, R., Vigliano, C., Lococo, B., Alvarez, M.G., Petti, M., Bertocchi, G., Armenti, A., 2009. Side effects of benznidazole as treatment in chronic Chagas disease: fears and realities. Expert Rev. Anti Infect. Ther. 7 (2), 157–163.

WHO, 2011. Informal Consultation on Chagas Disease in the Western Pacific. Manila, Philippines.

Yardley, V., Croft, S.L., 1999. *In vitro* and *in vivo* activity of amphotericin B-lipid formulations against experimental *Trypanosoma cruzi* infections. Am. J. Trop. Med. Hyg. 61 (2), 193–197.

Zingales, B., Andrade, S.G., Briones, M.R., Campbell, D.A., Chiari, E., Fernandes, O., Guhl, F., Lages-Silva, E., Macedo, A.M., Machado, C.R., Miles, M.A., Romanha, A.J., Sturm, N.R., Tibayrenc, M., Schijman, A.G., Meeting, S.S., 2009. A new consensus for *Trypanosoma cruzi* intraspecific nomenclature: second revision meeting recommends TcI to TcVI. Mem. Inst. Oswaldo Cruz 104 (7), 1051–1054.

Zingales, B., Miles, M.A., Moraes, C.B., Luquetti, A., Guhl, F., Schijman, A.G., Ribeiro, I., 2014. Drug discovery for Chagas disease should consider *Trypanosoma cruzi* strain diversity. Mem. Inst. Oswaldo Cruz 109 (6), 828–833.